Article

Not peer-reviewed version

Antioxidant Nanohybrid Materials Derived via Olive Leaves Extract Incorporation in Layered Double Hydroxide: Preparation, Characterization, and Evaluation for Applications

Achilleas Kechagias , Areti A. Leontiou , Alexios Vardakas , Panagiotis Stathopoulos , Maria Xenaki , Panagiota Stathopoulou , Charalampos Proestos , Emmanuel P Giannelis * , Nikolaos Chalmpes * , Constantinos E Salmas * , Aris E Giannakas *

Posted Date: 25 June 2025

doi: 10.20944/preprints202506.2137.v1

Keywords: olive leave extract; layered double hydroxide; antioxidant nanohybrids; total polyphenol content; enzymatic assisted extraction; 3 Hydroxytyrosol; Oleuropein; Luteolin-7-O-glucoside; Apigenin-4-O-glucoside

 doi:10.20944/preprints202506.2137.v1

Article

Antioxidant Nanohybrid Materials Derived Via Olive Leaves Extract Incorporation in Layered Double Hydroxide: Preparation, Characterization, and Evaluation for Applications

Achilleas Kechagias [1], Areti A. Leontiou [1], Alexios Vardakas [1,2], Panagiotis Stathopoulos [3], Maria Xenaki [4], Panayiota Stathopoulou [5], Charalampos Proestos [6], Emmanuel P. Giannelis [7], Nikolaos Chalmpes [7,*], Constantinos E. Salmas [7,8*] and Aris E. Giannakas [1,*]

[1] Department of Food Science and Technology, University of Patras, 30100 Agrinio, Greece
[2] GAEA Products S.M. S.A., 1st km Agriniou-Karpenissiou National Rd., GR-30100 Agrinio, Greece
[3] Division of Pharmacognosy and Natural Products Chemistry, Department of Pharmacy, National and Kapodistrian University of Athens, Athens, Greece
[4] PharmaGnose S.A., Papathanasiou 24, 34100 Chalkida, Greece
[5] Department of Sustainable Agriculture, University of Patras, 30100 Agrinio, Greece
[6] Laboratory of Food Chemistry, Department of Chemistry, National and Kapodistrian University of Athens Zografou, 15771 Athens, Greece
[7] Department of Materials Science and Engineering, Cornell University, Ithaca, New York 14850, USA
[8] Department of Material Science and Engineering, University of Ioannina, 45110 Ioannina, Greece
* Correspondence: agiannakas@upatras.gr (A.E.G.); ksalmas@uoi.gr (C.E.S.), nc427@cornell.edu (N.C.)

Abstract: In this study, an innovative approach for the valorization of olive leaves—an underutilized agro-industrial by-product—was employed through enzymatic-assisted aqueous extraction to obtain a polyphenol-rich olive leaf extract (OLE). The extract was found to contain significant levels of hydroxytyrosol (0.53 mg/L), luteolin-7-O-glucoside (0.70 mg/L), apigenin-4-O-glucoside (0.18 mg/L), and oleuropein (4.24 mg/L). For the first time, this OLE was successfully nanoencapsulated into layered double hydroxides (LDHs) synthesized at three Zn^{2+}/Al^{3+} molar ratios (1:1, 2:1, and 3:1) to form OLE@LDH_Zn/Al_x/1 nanohybrids. The hybrids were thoroughly characterized by XRD, FTIR, and SEM, confirming the intercalation of OLE into the LDH interlayer structure. Antioxidant activity (via DPPH assay), total polyphenol content (TPC), and antibacterial tests (disk diffusion, MIC, and MBC) were conducted to evaluate functionality. Among the nanohybrids, OLE@LDH_Zn/Al_1/1 exhibited the highest TPC (606.6 ± 7.0 mg GAE/L), the lowest EC_{50} (83.64 ± 5.45 μg/mL), and superior antibacterial performance against *E. coli* and *S. aureus*. Moreover, pH-dependent release profiles confirmed targeted release at acidic conditions (pH 1), simulating gastric environments. These findings suggest that LDHs, especially with a Zn/Al ratio of 1:1, are promising carriers for the stabilization and controlled release of bioactive polyphenols in nutritional and biomedical applications.

Keywords: olive leave extract; layered double hydroxide; antioxidant nanohybrids; total polyphenol content; enzymatic assisted extraction; 3 Hydroxytyrosol; Oleuropein; Luteolin-7-O-glucoside; Apigenin-4-O-glucoside

1. Introduction

In recent years, global trends in bioeconomy and sustainability have driven scientists and researchers to develop "green" technologies aimed at reducing carbon dioxide emissions and minimizing reliance on fossil fuels, and decreasing food waste [1–5]. In alignment with these priorities, biomass valorization, the utilization of food and agricultural by products and side streams,

 doi:10.20944/preprints202506.2137.v1

and the reduction of food waste have become areas of significant scientific focus [6–12]. In the field of Food Technology, these efforts are primarily centered on the recovery of biopolymers from biomass as sustainable alternatives to fossil fuel-derived plastics, as well as th extraction of bioactive compounds for use in functional foods and biobased preservatives [9,13,14]. Among the most prominent categories of bioactive compounds are natural extracts and essential oils (EOs)[15–20] which exhibit antioxidant, antibacterial, antifungal and anticancer properties rendering them highly promising for applications in food preservation and nutrition [15,18–20]. To enhance the efficacy and control the release of these compounds encapsulation within cost-effective nanocarriers such as layered silicates, and natural zeolites has been proposed [20–25].

Layered silicates include naturally abundant nanoclays like montmorillonite and halloysite, as well as synthetically produced layered double hydroxides (LDHs). The key difference between these materials lies in their ion exchange capabilities: LDHs primarily intercalate negatively charged ions, while natural nanoclays typically intercalate positively charged cations [26–28]. Both LDHs and nanoclays have been extensively studied in recent years as nanocarriers for bioactive compounds [25,29,30]. LDHs, which are two-dimensional (2D) clay materials of the Hydrotalcite (HTs) type,are particularly suitable for intercalating bioactive molecules within their interlayer spaces [25]. These materials can be dispersed within polymeric matrices, enabling the incorporation of phenolics, polyphenols and other bioactive compounds. LDHs offer several advantages including low cost, high biocompatibility, non-toxicity, pH-dependent stability, controlled release behavior , high anion exchange capacity, low surface charge and excellent thermal andchemical stability [25,31]. Various bioactive anions such as salicylate, d-gluconate, citrate, l-ascorbic, and cinnamate have been successfully intercalated into LDHs to form LDH/bioactive hybrids with antioxidant and antibacterial properties, suitable for use in food preservation either directly or embedded in polymeric or biopolymeric matrices [32–40]. To the best of our knowledge, polyphenols derived from olive oil or olive tree leaves have not previously been reported as intercalated compounds in LDHs. Encapsulation of such biologically active molecules within LDHs layers may serve as a protective “chemical flask jacket”, shielding them from biodegradation while facilitating improved cellular uptake [41].

Olive tree leaves, a by-product of olive oil production, are typically discarded despite being a rich source of bioactive compounds [42,43]. These leaves contain high concentrations of valuable polyphenols including 3 Hydroxytyrosol (HT), Oleuropein (Oleur), Luteolin-7-O-glucoside (Lut-7-O-glu) and Apigenin-4-O-glucoside (Apig-4-O-glu) [42]. Recovering these health-promoting compounds supports their use in cosmetics, biomedicine and the food industry as dietary supplements or natural additives [42]. Recent studies have demonstrated the successful valorization of olive tree leaves using environmentally friendly extraction methods, such as enzyme-assisted methods, to obtain olive leaf extract (OLE) a total polyphenol content up to 605.55 mg GAE/L and high antioxidant activity [44].

Herein, we report for the first time the successful intercalation and encapsulation of oleuropein-rich OLE into Zn-Al based layered double hydroxides (LDH_Zn/Al). LDHs were synthesized using three different Zn^{2+}: Al^{3+} ratios- (1:1, 2:1, and 3:1)- resulting in the materials named LDH_Zn/Al_1_1, LDH_Zn/Al_2_1, and LDH_Zn/Al_3_1, respectively. The corresponding nanohybrids, OLE@LDH_Zn/Al_x/1 (x=3, 2, 1) were thoroughly characterized using X-ray diffraction (XRD), Fourier Transform Infrared (FTIR) Spectroscopy, High Resolution Scanning Electron Microscopy (HR-SEM) and N_2 porosimetry. The antioxidant activity of the OLE@LDH_Zn/Al nanohybrids was assessed via the 2,2-diphenyl-1-picrylhydrazyl (DPPH) assay. Antibacterial activity was tested against *Escherichia coli* and *Staphylococcus Aureus* and controlled release experiments were conducted to evaluate the release profile of OLE.. This comprehensive study aims to identify the most effective OLE@LDH_Zn/Al nanohybrid for potential applications in nutrition and/or biomedicine as a controlled release nanocarrier for bioactive polyphenols.

2. Materials and Methods

 doi:10.20944/preprints202506.2137.v1

2.1 Materials

$Zn(NO_3)_2x6H_2O$, $Al(NO_3)_3x9H_2O$, and NaOH were purchased from Sigma-Aldrich (Darmstadt, Germany). For analytical purposes, 2,2-Diphenyl-1-picrylhydrazyl (DPPH·), absolute ethanol (C_2H_5OH), sodium carbonate (Na_2CO_3), and acetate buffer ($CH_3COONa \times 3H_2O$) were purchased from Sigma-Aldrich (Darmstadt, Germany) while Folin–Ciocalteu reagent from Sigma-Aldrich; and gallic acid (3,4,5-trihydrobenzoic acid) 99% isolated from Rhus chinensis Mill (JNK Tech. Co., Seongnam, Republic of Korea). All solvents were HPLC grade; acetonitrile (99.9 % purity), water (≥99.9 % purity), methanol (>99.8 % purity), were obtained from ChemLab (Zeldegem, Belgium). HT reference standard was purchased from ExtraSynthase (Lyon Nord, France), while the Lut-7-O-glu, Apig-4-O-Glu and Oleur reference standards were purchased from Sigma Aldrich (Darmstadt, Germany). Olive (Olea europaea) leaves, Koroneiki variety harvested year 2023, were obtained from a producer in the region of Agrinio, Greece. The leaves were dried at 50 ◦C for 5 h.

2.2. Enzymatic Assisted Extraction

The enzymatic-assisted extraction of OLE was conducted according to our recent study and is described in detail in the supplementary material file [40].

2.3 OLE@LDH_Zn/Al Nanohybrids Preparation

Firstly, 50 ml of OLE was filtered under vacuum. An 8M aqueous NaOH solution was prepared by dissolving 9.6 g of NaOH pellets in 30 ml of purified water. To achieve final Zn/Al ratios of 1:1, 2:1 and 3:1, the appropriate amounts of $Zn(NO_3)_2$ $6H_2O$ and $Al(NO_3)_3$ $9H_2O$ salts were accurately weighed using an analytical balance. Subsequently, the weighed salts were then added to 10 ml of purified water in a 250ml beaker and stirred until completely dissolved. Once dissolution was complete, the beaker was transferred to a chemical fume hood in an oil bath at 60 °C, under continuous stirring. When the solution reached 60 °C, the filtered OLE was added and stirring continued until temperature stabilized. The previously prepared NaOH solution was then added dropwise to the mixture until the pH reached 7. The reaction mixture was maintained at 60 °C with constant stirring for 24 h. After this period, the suspension was transferred into two centrifuge tubes and centrifuged 3 times at 3000 rounds per minute (rpm) for 2-4 min. After the first centrifugation, the pale-yellow supernatant was discarded. A small amount of purified water was added to the sediment, followed by manual stirring and 3 minutes of ultrasonic treatment. The tubes were then refilled with purified water prior to the second centrifugation. This washing process was repeated for each centrifugation step, although sonication was only performed after the first wash. Following the third centrifugation, the supernatant – now colorless and transparent- was discarded. The remaining sediment was resuspended in a small volume of purified water, manually stirred, and transferred to a glass plate to maximize recovery. The final product, OLE@LDH_Zn/Al nanohybrid, was dried overnight at 40 °C.

2.4 Phytochemical Analyses of OLE

The determination of HT, Lut-7-O-Glu, Apig-4-O-Glu and Oleur in the Olive leaf extract was performed following the analytical method proposed by the IOC, in accordance with the conditions described in IOC/T.20/Doc No 29 method [45]. Specifically, component separation was achieved using a reversed-phase Discovery HS C18 column (250 × 4.6 mm, 5 µm). The mobile phase consisted of 0.2% aqueous orthophosphoric acid (solvent A) and a methanol/acetonitrile mixture (50:50 v/v), as solvent B. Chromatographic separation was carried out at ambient temperature with a flow rate of 1.0 mL/min and an injection volume of 20 µL. The gradient elution was as follows: 0 min, 96% A and 4% B; 40 min, 50% A and 50% B; 45 min, 40% A and 60% B; 60 min, 0% A and 100% B; 70 min, 0% A and 100% B; 72 min, 96% A and 4% B; 82 min, 96% A and 4% B. Chromatograms were monitored at 280 nm.

 doi:10.20944/preprints202506.2137.v1

Quantification of the major compounds was achieved using regression analysis. Calibration curves were constructed for each standard compound. For HT and Lut-7-O-Glu, 9-point calibration curves were used: (HT: y = 87594x + 31144, r^2 = 0.9999; Lut-7-O-Glu: y = 123082x - 14814, r^2 = 0.9996.), while Apig-4-O-Glu and Oleur quantified according to 8-points calibration curve, respectively (Apig-4-O-Glu: y = 245381x - 42718, r2 = 0.9997; Oleur: y = 22405x + 313038, r^2 = 0.9982).

2.5. Physicochemical Characterization of OLE@LDH_Zn/Al_x/1 Nanohybrids

The synthesized OLE@LDH_Zn/Al_x/1 nanohybrids were characterized using X-Ray Diffraction (XRD), Fourier Transform Infrared Spectroscopy (FTIR) and Scanning Electron Microscopy (SEM). Details of the instrumentation and methodologies used for the XRD, FTIR and SEM analyses are provided in supplementary material file in detail.

2.6. Antioxidant Activity of OLE@LDH_Zn/Al_x/1 Nanohybrids

For all OLE@LDH_Zn/Al_x/1 nanohybrids, as well as pure freeze-dried OLE the concentration required to achieve a 50% antioxidant effect (EC_{50}) was determined using the 2,2-diphenyl-1-picrylhydrazyl (DPPH) assay by following the methodology described in supplementary material file in detail.

2.7. Total Polyphenols Content (TPC) of OLE@LDH_Zn/Al_x/1 Nanohybrids

The TPC of obtained OLE and all the obtained Zn/Al_x/1 nanohybrids was measured by using a SHIMADJU UV/VIS spectrophotometer (UV-1900, Kyoto, Japan) via the following methodology.

TPC of OLE: 0.2 mL of OLE were added in a 5 mL volumetric flask along with 2.5 mL of distilled water and 0.25 mL of Folin-Ciocalteü reagent. After 3 min, 0.5 mL of saturated sodium carbonate (Na_2CO_3, 30% w/v) was also added into the mixture. Finally, the solution obtained was adjusted to 5 mL using distilled water for measurements at pH=7, with 1M citric acid aqueous solution for measurements at pH=3.6, and with 0.1M HCl aqueous solution for measurements at pH=1. The mixture was incubated in the dark at room temperature for 2 h after which the absorbance was measured at λ = 760 nm. The results were presented as equivalents of gallic acid (GAE). Each sample was analyzed in triplicate (n = 3).

TPC of Zn/Al_x/1 nanohybrids: 10 mg of each nanohybrid were added in 10 ml of ethanol. The mixture was stirred and filtered with 0.45 μm filters to obtain 10 mL of an ethanolic extraction. Then 0.20 mL of such ethanolic extraction were added in a 5 mL volumetric flask, 0.20 mL of the ethanolic extracts followed by the addition of 2.50 mL of distilled water and 0.25 mL of Folin-Ciocalteu reagent. After 3 min, 0.50 mL of saturated sodium carbonate (Na_2CO_3, 30% w/v) was also added into the mixture. Finally, the solution obtained was brought to 5 mL with distilled water for the mesuraments at pH=7, with 1M citric acid aquatic solution for measurements at pH=3.6, and with 0.1M HCl aquatic solution for measurements at pH=1. This solution was left for 2 h in the dark at room temperature and the absorbance was measured at λ = 760 nm. The results were presented as equivalents of gallic acid (GAE). Each sample was analyzed in triplicate (n = 3).

All TPC measurements were performed using 1 cm pathlength cuvettes.

2.8. Antibacterial Activity

2.8.1 Antimicrobial Activity of of OLE@LDH_Zn/Al_x/1 Nanohybrids

Standard and isolated strains of the following three bacteria, including one Gram-positive (*Staphylococcus aureus* (ATCC25923)) (*E. Coli*) and one Gram-negative (*Escherichia coli* (ATCC25922)) (*S. Aureus*) bacteria were used in screening the antimicrobial activity. The antimicrobial activity of the OLE@LDH_Zn/Al_x/1 nanohybrids was determined using the disk diffusion method according to EUCAST guidelines and the minimum inhibitory concentration (MIC) and minimum bactericidal concentration (MBC) was determined after applying the resazurin-based 96-well plate microdilution

 doi:10.20944/preprints202506.2137.v1

method [46]**.** MIC, MBC and ZOI (zone of inhibition) antibacterial activity mean values obtained after three repetitions of antibacterial activity tests.

2.8.2. Disk Diffusion Susceptibility Test

Aseptically, 50 mg of each of the OLE@LDH_Zn/Al_x/1 nanohybrids were weighed and directly applied as a defined circular deposit onto the surface of Mueller-Hinton agar (MHA) plates which had been previously inoculated with the respective test microorganism (108 CFU ml^{-1}). A minimum center-to-center distance of 24 mm was maintained between each sample application site to prevent overlapping of the inhibition zones. The inoculated MHA plates were then incubated at 37 °C for 24 h. After the incubation, the diameter of the clear zone of inhibition surrounding each disc was calculated using a calibrated ruler. The actual diameter of inhibition was then calculated by subtracting the initial diameter of the applied sample deposit from this measurement. Specifically, the actual inhibition diameter was calculated by subtracting the initial diameter of the applied sample deposit from this measurement. The test was performed in duplicate for each test microorganism and OLE@LDH_Zn/Al_x/1 nanohybrids concentration.

2.8.3. Resazurin-Based 96-Well Plate Microdilution Method

The MIC determination of OLE@LDH_Zn/Al_x/1 nanohybrids samples was performed following the protocol described by [46]. The analyses were carried out in a microdilution plate with 96 wells (see Figure S4) (sterilized, 300 µL capacity, MicroWell, NUNC, Thermo-FisherScientific, Waltham, MA). The OLE@LDH_Zn/Al_x/1 nanohybrids were dissolved in sterile dH_2O. Initial solutions of OLE@LDH_Zn/Al_x/1 nanohybrids were prepared at a concentration of 50 mg ml^{-1} and further serial dilutions were performed in the 96 well plate in Mueller-Hinton broth (MHB). The concentrations tested ranged from 25 to 0.05 mg. mL^{-1}. Positive controls (growth control) containing inoculum as well as negative controls with broth (MHB) were prepared. After adding a standardized inoculum of the target bacteria (108 CFU ml^{-1}), the microplate was then incubated for 24 h at 37 °C. After incubation, 50 µL of a 0.015% w/v resazurin solution was added to each well and the plate was incubated for another 2 hours. If there's no metabolic activity (inhibition) the Resazurin stays blue and if there is activity (growth) turns pink/purple. Wells without color change were scored as concentrations above the MIC. Treatments that showed inhibition of microorganisms were then tested for bactericidal activity (MBC) by plating a 10 µL sample onto MHA plates and incubating for 24 hours at 37 °C. The lowest treatment concentration that did not show colony formation after incubation in all replicates was considered the MBC.

2.9. Statistical Analysis

Descriptive statistics for OLE extraction yield, hydroxytyrosol content, luteolin-7-glycoside content, and Oleuropein content, as well as for EC_{50}, TPC, and ZOI parameters were estimated using SPSS software (version 29.0; IBM Corp., Armonk, NY, USA). The last three properties were also subjected to statistical analysis to investigate the statistically significant differences of their mean values. For such investigation the statistical test method ANOVA was chosen. A significance level of $p < 0.05$ was adopted for all comparisons.

3. Results

3.1. HPLC-DAD Analyses of OLE

The results of the phytochemical analysis, including the mean values of total polyphenols extraction yield, hydroxytyrosol content, luteolin-7-glycoside content and Hydroxytyrosol, Luteolin-7-O-glucoside, Apigenin-4-O-glucoside and Oleuropein content of the sample OLE, obtained from HPLC-DAD analysis, are summarized in Table 1. These values were calculated by using the calibration curves of Hydroxytyrosol, Luteolin-7-O-glucoside, Apigenin-4-O-glucoside and Oleuropein

 doi:10.20944/preprints202506.2137.v1

presented in Figure S2 and obtained HPLC-DAD chromatogram at 280 nm for pure OLE of Figure S2.

Table 1. Phytochemical analysis of pure OLE

Sample name	Extraction yield (mg/L)	hydroxytyrosol (mg/L)	luteolin-7-glycoside (mg/L)	Apigenin-4-O-glucoside (mg/L)	Oleuropein (mg/L)
OLE	24.00±0.02	0.53±0.02	0.70±0.02	0.18±0.01	4.24±0.03

As shown in Table 1 a high extraction yield of 24.0 ± 2.8 mg/L was obtained for the pure OLE. This high extraction yield value is attributed to the optimum combination of Viscozyme and pectinolytic enzymes used in the microwave-assisted extraction process [44]. According to the HPLC-DAD analysis results presented in Table 1, the pure OLE contains 2.19%wt. Hydroxytyrosol (0.53mg/L), 2.89%wt. Luteolin-7-O-glucoside (0.70 mg/L), 0.75%wt. Apigenin-4O-glucoside and 17.64 %wt. Oleuropein (4.24 mg/L). These findings indicate that pure OLE is rich in total polyphenols with approximately 25%wt. consisting of high-value polyphenolic compounds such as Hydroxytyrosol, Luteolin-7-O-glucoside, Apigenin-4-O-glucoside and Oleuropein.

3.2 Physicochemical Characterization of OLE@LDH_Zn/Al_x/1 Nanohybrids

3.2.1 XRD analysis of OLE@LDH_Zn/Al_x/1 nanohybrids

Figure 1 presents the XRD patterns of all synthesized OLE@LDH_Zn/Al_x/1 nanohybrids, along with that of pure LDH_$NaNO_3$_Zn/Al for comparison.

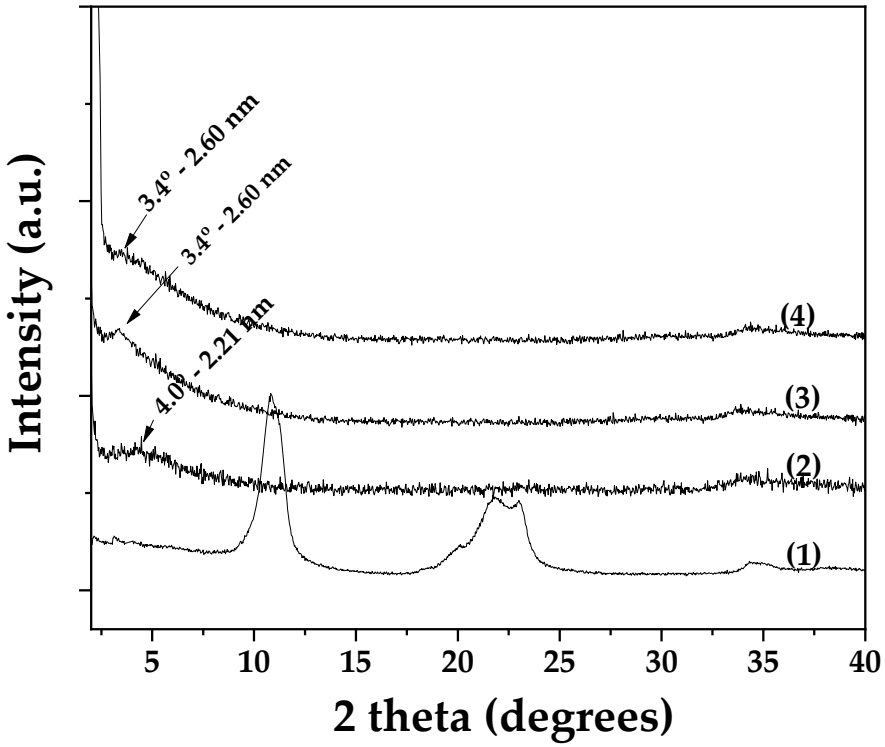

Figure 1. XRD patterns of (1) pure LDH_$NaNO_3$_Zn/Al, (2) OLE@LDH_Zn/Al_1/1, (3) OLE@LDH_Zn/Al_2/1, AND (4) OLE@LDH_Zn/Al_3/1.

 doi:10.20944/preprints202506.2137.v1

As shown in Figure 1 and in agreement with previous reports, the characteristic (003) reflection of pure LDH_NaNO$_3$_Zn/Al (plot line (1)) appears at approximately 10^o, corresponding to a basal spacing of 0.83 nm [47,48]. In all XRD patterns of the OLE@LDH_Zn/Al_x/1 nanohybrids, a broad peak around 5^o indicates that the (003) reflection of LDH has shifted to lower angles. Specifically, the basal space increases to 2.21 nm for OLE@LDH_Zn/Al_1/1 (plot line (2)), and to 2.60 nm for both OLE@LDH_Zn/Al_2/1 (plot line (3)), and OLE@LDH_Zn/Al_3/1 (plot line (4)) nanohybrids. This small differentiation in the observed basal space of obtained OLE@LDH_Zn/Al_x/1 nanohybrids suggest different orientation of intercalated OLE molecules inside the interlayer space of LDH rather correlation with the OLE adsorbed amount [49,50]. Among the three LDH nanohybrids, OLE@LDH_Zn/Al_2/1 exhibits the most intense (003) reflection, suggesting the best platelet orientation. Overall, the XRD results confirm the successful intercalation of OLE molecules into the LDH the interlayer space.

3.2.2. FTIR of OLE@LDH_Zn/Al_x/1 Nanohybrids

Figure 2 displays the FTIR spectra of all synthesized OLE@LDH_Zn/Al_x/1 nanohybrids, along with those of pure LDH_NaNO$_3$_Zn/Al and pure OLE for comparison.

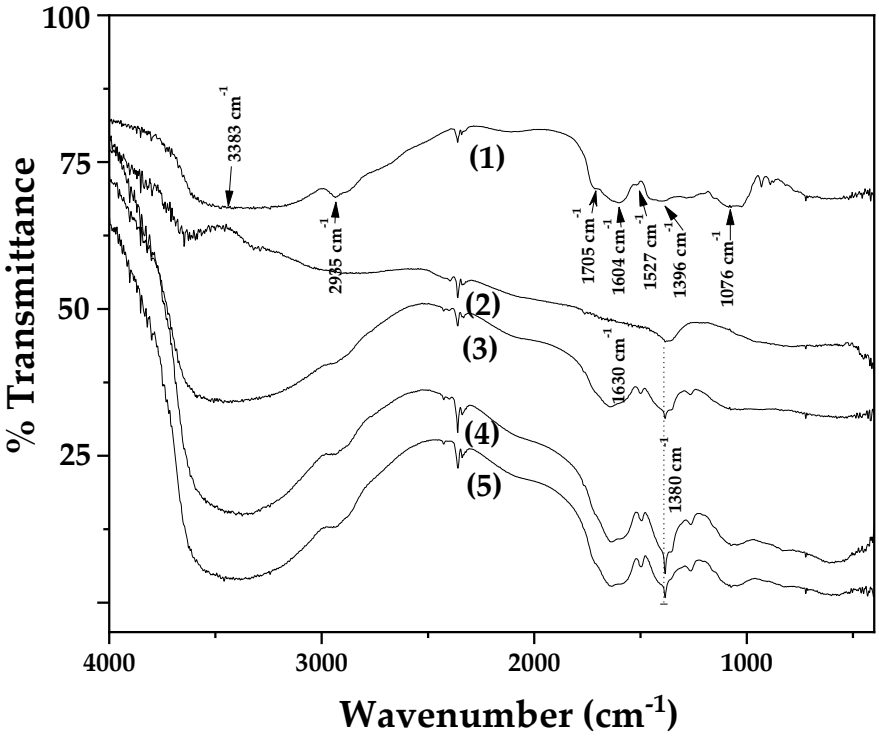

Figure 2. FTIR plots of (1) pure OLE, (2) pure LDH_NaNO$_3$_Zn/Al, (3) OLE@LDH_Zn/Al_1/1, (4) OLE@LDH_Zn/Al_2/1, AND (5) OLE@LDH_Zn/Al_3/1.

The FTIR spectrum of pure OLE (plot line (1) displays several absorption peaks, reflecting its complex chemical composition. The peak at 3383 cm^{-1} can be attributed to the N–H stretching vibration of amino groups and also indicates the presence of bonded hydroxyl (-OH) group [51]. The absorption peak at 2935 cm^{-1} corresponds to –CH stretching vibrations of both –CH$_3$ and –CH$_2$ functional groups [51–54]. The shoulder peak at 1705 cm^{-1} is assigned to the C=O stretching vibration of carboxylic acids. These two prominent bands at 3383 and 1705 cm^{-1} are characteristic of the O–H and C=O stretching modes, potentially originating from compounds such as Oleuropein, Apigenin-4-O-glucoside and/or Luteolin-7-O-glucoside [51,52,55,56]. The peak at 1604 cm^{-1} lies within the fingerprint region and is associated with the presence of CO, C–O and O–H functional groups found in OLE [4]. Specifically, it can be attributed to C–O stretching in carboxyl groups coupled with the

 doi:10.20944/preprints202506.2137.v1

amide I linkage. The band at 1527 cm^{-1}, characteristic of amide II arises from N-H stretching modes in the amide linkage [57]. The peak at 1396 cm^{-1} is attributed to methylene scissoring vibrations associated with protein content. A strong band at 1076 cm^{-1} is assigned to C-N stretching vibrations of aliphatic amines or C-OH vibrations in proteins derived from olive leaves [51,52,55,56,58].

In the FTIR spectra of all synthesized LDHs (plot lines (2), (3), (4), and (5)) characteristic bands of hydrotalcite-like compounds are revealed. The broad and intense band centered at 3620 cm^{-1} is attributed to the stretching of the OH groups and adsorbed H_2O molecules [59]. region between 603 - 430 cm^{-1} corresponds to Al-O and Zn-O vibrational modes [59]. A weak band at 1630 cm^{-1} is attributed to the bending vibration of interlayer water molecules. [59]. The FTIR spectrum of Zn-Al-NO_3 reveals a strong peak near 1380 cm^{-1} , corresponding to the antisymmetric stretching mode (v_3) of nitrate anions present in the LDH structure [59]. Comparing the FTIR spectra of pure LDH_$NaNO_3$_Zn/Al with those of all OLE@LDH_Zn/Al_x/1 nanohybrids reveals a significant difference: a large, broad peak around 3500 cm^{-1} appears in all nanohybrid spectra. This peak results from overlapping hydroxyl group vibrations from both the LDH and OLE, indicating strong interactions between the intercalated hydroxyl groups of OLE and the internal hydroxyl groups of the LDH platelets.

3.2.3. HR-SEM analysis of OLE@LDH_Zn/Al_x/1 Nanohybrids

The morphological characteristics of pure OLE and LDH along with the corresponding nanohybrids are presented in Figure 3.

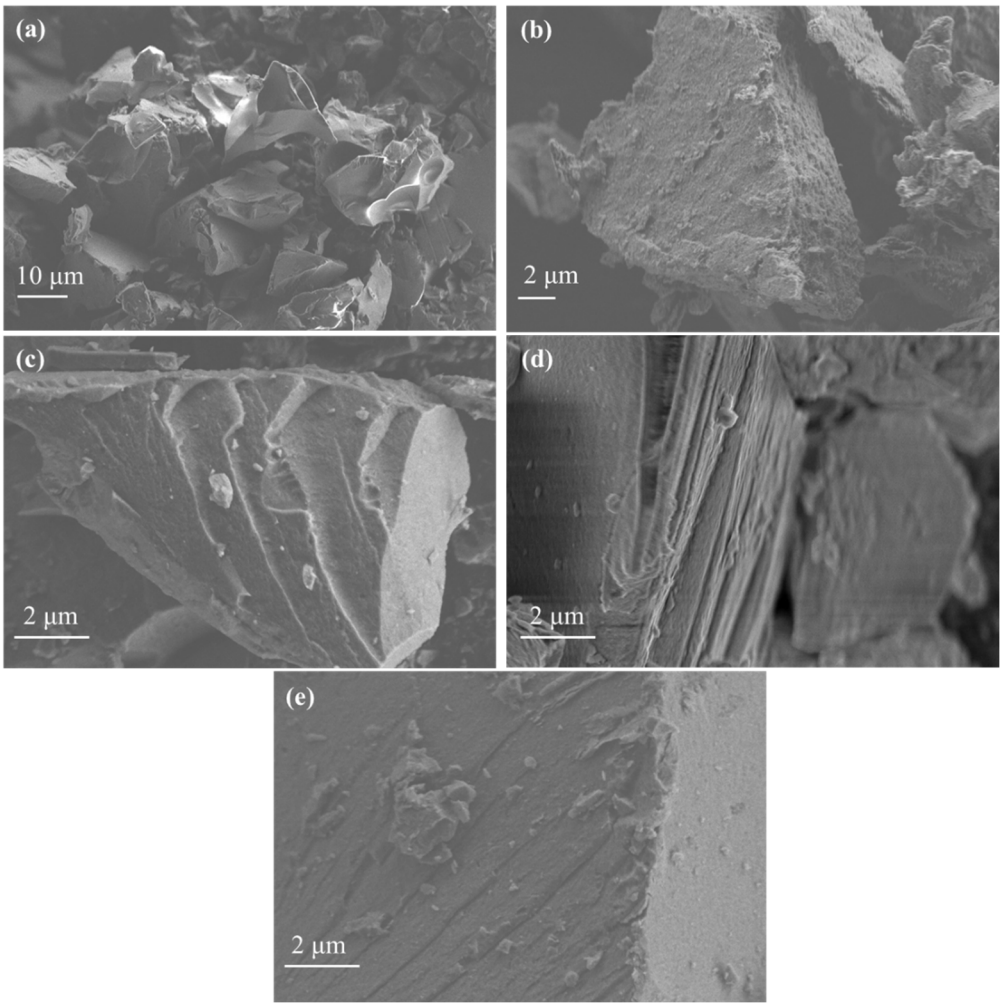

Figure 3. SEM images of (a) pure freeze-dried OLE, (b) pure LDH_$NaNO_3$_Zn/Al, (c) OLE@LDH_Zn/Al_1/1, (d) OLE@LDH_Zn/Al_2/1, AND (e) OLE@LDH_Zn/Al_3/1

 doi:10.20944/preprints202506.2137.v1

Representative images of pure freeze-dried OLE and LDH are shown in Figures 3a and 3b, respectively. Pure freeze-dried OLE structure has a sponge-like structure with large holes which indicate the evaporated water molecules. Pure LDH structure reveal an irregular disk-like or flakes-like morphology with obvious lamellar structure, which is a typical characteristic of LDH nanostructures [60,61]. Larger platelets or clusters of LDH are also observed indicating their tendency to agglomerate or overlap due to interlayer forces and particle-particle interactions [61,62]. The SEM images of LDH-modified nanohybrids (see images in Figure 3c, d, and e) reveal notable morphological changes compared to the unmodified nanostructures. In all OLE@LDH_Zn/Al_x/1 nanohybrids, large sandwich-like particles are observed, suggesting successful OLE intercalation and particle agglomeration. Additionally, irregular nanostructures or particles appear on the surface of the LDH layers, which can be attributed to the OLE nanostructure. Among the nanohybrids, the sandwich-like morphology is most pronounced in OLE@LDH_Zn/Al_2/1. This observation is consistent with the XRD results, which indicate that the most favorable platelet orientation occurs in the OLE@LDH_Zn/Al_2/1 nanohybrid.

3.3. Antioxidant Activity of OLE@LDH_Zn/Al_x/1 Nanohybrids

Antioxidant activity of all obtained OLE@LDH_Zn/Al_x/1 nanohybrids as well as pure OLE was evaluated via DPPH assay method and the determination of effective concentration for 50% antioxidant activity (EC_{50}). Calculated mean values of EC_{50} are plotted in Figure 4 for comparison.

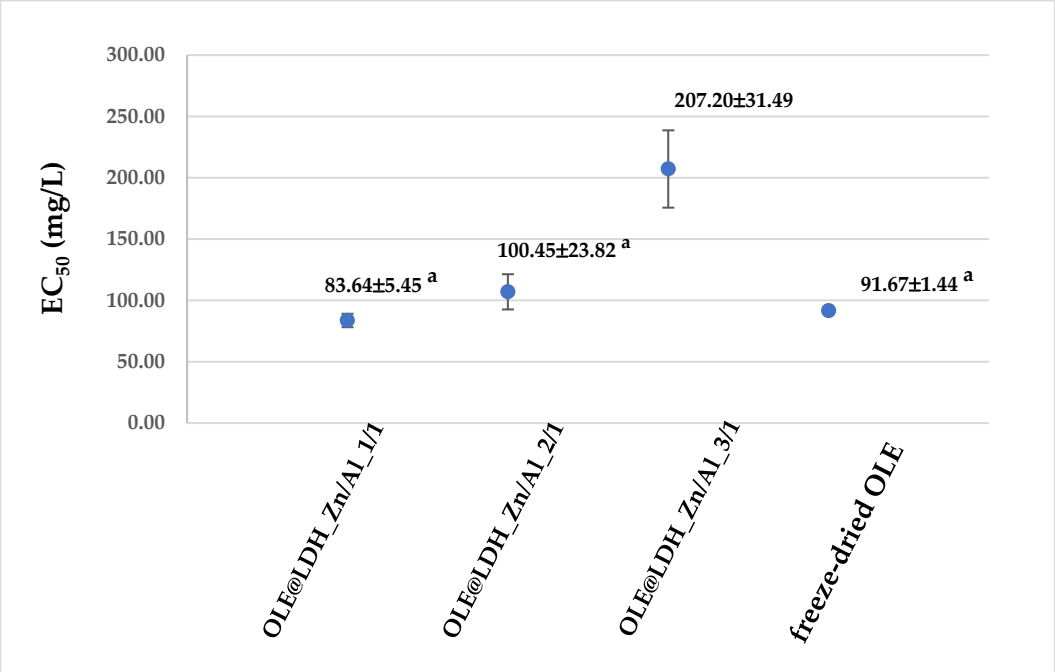

Figure 4. Plot with calculated mean and standard deviation values of EC_{50} all OLE@LDH_Zn/Al_x/1 nanohybrids as well as pure freeze-dried OLE. Different letters in each bar indicate statistically significant differences at a confidence level of $p < 0.05$. See also Table S2 in supplementary material file.

As shown in Figure 4 for OLE@LDH_Zn/Al_1/1 nanohybrid the obtained EC_{50} value is 83.64±5.45, for OLE@LDH_Zn/Al_2/1 nanohybrid the obtained EC_{50} value is 100.45±23.82, and for OLE@LDH_Zn/Al_3/1 nanohybrid the obtained EC_{50} value is 207.204±31.49. In other words, as the Zn/Al molar ratio increases the obtained EC_{50} values increase too or the antioxidant activity decreases. As the Zn ion content decrease the obtained LDH_Zn/Al sheet becomes more positive [63,64]. More positive sheets of LDH can intercalate more negative charged OLE amount and thus obtained OLE@LDH_Zn/Al_1/1 nanohybrids has the highest antioxidant capacity. Zn/Al molar ratio is well know that effects the photocatalytic, optical, and dielectric properties of such Zn-Al-LDH [65]. Herein, it is for the first time reported that this Zn/Al molar ration is crucial also for the antioxidant

 doi:10.20944/preprints202506.2137.v1

capacity of obtained OLE@LDH_Zn/Al_x/1 nanohybrids. In addition, as it is obtained in Figure 4 OLE@LDH_Zn/Al_1/1 nanohybrid has higher antioxidant capacity than pure freeze-dried OLE. This probably reveals a synergistic effect between antioxidant activity of nanoencapsulated OLE polyphenols inside the sheets of LDH and the Zn/Al ions antioxidant activity.

3.4. Total polyphenols Content (TPC) of OLE@LDH_Zn/Al_x/1 Nanohybrids

In Figure 5 are plotted the calculated mean TPC values of all obtained OLE@LDH_Zn/Al_x/1 nanohybrids in pH=7, 3.6, and 1.

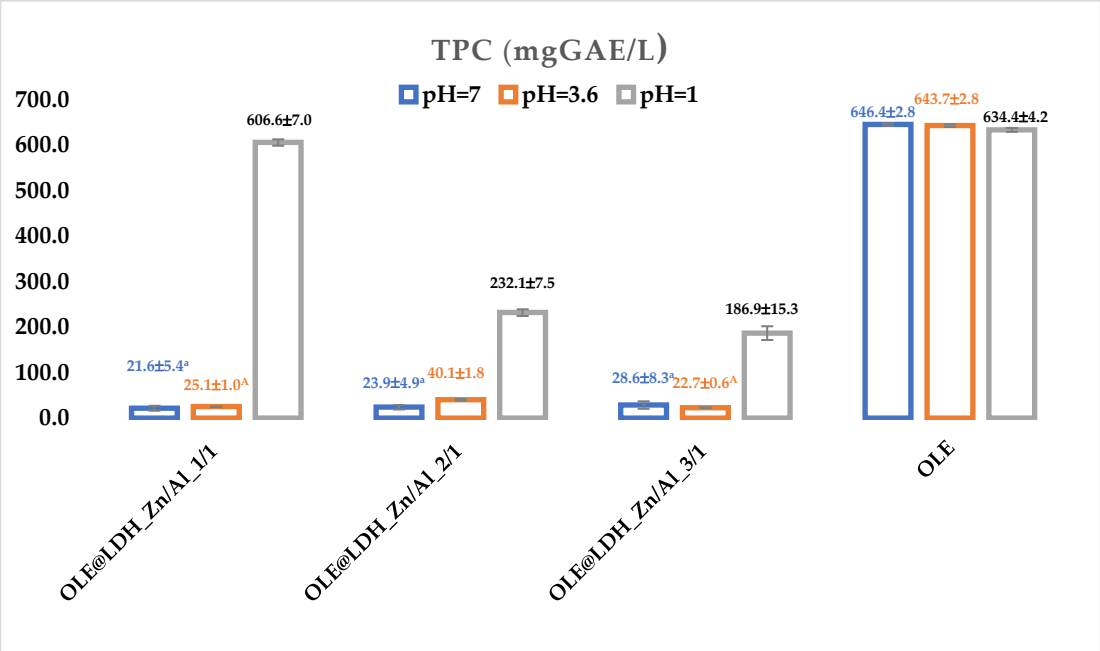

Figure 5. Calculated mean TPC values of all obtained OLE@LDH_Zn/Al_x/1 nanohybrids in pH=7, 3.6, and 1 as well as pure OLE. Different letters (a,A) in each bar indicate statistically significant differences at a confidence level of $p < 0.05$. See also Table S3 in supplementary material file.

As it is observed in Figure 5 pure OLE has high mean TPC values equal to 646.4±2.8, 643.7±2.8, and 634.4±4.2 at 7, 3.6, and 1 pH values correspondingly. On the other hand, for all OLE@LDH_Zn/Al_x/1 nanohybrids for both 7 and 3.6 pH values the obtained TPC values are very low. At pH=1 the observed means TPC values are much higher than these at 7, 3.6 pH values for all nanohybrids. Thus, 606.6±7.0, 232.1±7.5, and 186.9±15.3 mgGAE/L mean values are observed for OLE@LDH_Zn/Al_1/1, OLE@LDH_Zn/Al_2/1, and OLE@LDH_Zn/Al_3/1 correspondingly. The obtained low TPC values for all OLE@LDH_Zn/Al_x/1 nanohybrids at 7 and 3.6 pH is a direct proof that OLE polyphenols have been successfully nano-encapsulated inside the interlayer space of LDH's and cannot release to be detected. On the other hand, when pH fellows down to pH=1 the LDH sheets open/diluted and free the encapsulated OLE polyphenols and thus OLE polyphenols are detectable. This result validating the potential application of such OLE@LDH_Zn/Al_x/1 nanohybrids in nutrition and or medicine and clearly show that the encapsulated OLE polyphenols are well protected within the LDH's sheets and are released at a pH equal to the pH of stomach (pH ~1.2-1.8). In the acidic environment of the stomach, polyphenols are generally stable and undergo minimal hydrolysis or absorption [66,67]. In addition, the TPC results are in accordance with the antioxidant activity results hereabove. Obtained mean TPC values and EC_{50} values of all OLE@LDH_Zn/Al_x/1 nanohybrids increase with the same trend. The highest TPC and EC_{50} values are obtained for OLE@LDH_Zn/Al_1/1 nanohybrid. This means that the OLE@LDH_Zn/Al_1/1 nanohybrid which is the highest charged one encapsulates the highest amount of OLE polyphenols and thus exhibits the highest antioxidant capacity.

 doi:10.20944/preprints202506.2137.v1

3.5. Antibacterial Activity of OLE@LDH_Zn/Al_x/1 Nanohybrids

Results of antibacterial activity of all obtained OLE@LDH_Zn/Al_x/1 nanohybrids against *E. Coli* and *S. Aureus* via the disk diffusion method (ZOI), the minimum inhibitory concentration (MIC), and the minimum bactericidal concentration (MBC) are listed in Table 2 for comparison.

Table 2. Comparison of antimicrobial activities from OLE@LDH_Zn/Al_x/1 against E. Coli and S. Aureus via the disk diffusion method (ZOI), the minimum inhibitory concentration (MIC) method, and the minimum bactericidal concentration (MBC) method.

Bacteria	Sample	MIC (mg/mL)	MBC (mg/mL)	ZOI (mm)
E.coli				
	1/1	3.12	12.5	5±1[a]
	2/1	3.12	6.25	6±1[a]
	3/1	3.12	6.25	6±1[a]
S. aureus				
	1/1	1.56	6.25	3±1[b]
	2/1	0.78	6.25	4±1[b]
	3/1	1.56	3.12	4±1[b]

1/1: OLE@LDH_Zn/Al_1/1; 2/1: OLE@LDH_Zn/Al_2/1; 3/1: OLE@LDH_Zn/Al_3/1; MIC: minimum inhibitory concentration after three repetitions; MBC: minimum bactericidal concentration after three repetitions; ZOI: zone of inhibition; see also Figure S4 in supplementary material file.

As denoted in Table 2 all *OLE@LDH_Zn/Al_x/1* nanohybrids exhibited significant antibacterial activity against both *E. Coli* and *S. Aureus* via the disk diffusion method (ZOI), the minimum inhibitory concentration (MIC), and the minimum bactericidal concentration (MBC). Antibacterial results aligning with similar reports were OLE was encapsulated in maltodextrin based and maltodextrin/casein based formulas and exhibited significant antibacterial activity against various both Gram positive and gram negative bacteria [68,69]. Among the three methods used to determine the antimicrobial capacity of hybrids, the MIC and MBC methods are more reliable for comparative conclusions [70,71]. Thus, according to both MIC and MBC results listed in Table 2 OLE@LDH_Zn/Al_1/1 nanohybrid exhibited the highest antibacterial activity against both *E. Coli* and *S. Aureus*. This result aligning with the highest TPC value and the highest EC_{50} value of OLE@LDH_Zn/Al_1/1 nanohybrid and validating the current study.

4. Discussion

In this study olive leaves valorization was achieved through an environmentally friendly enzymatic assisted extraction method, yielding an aqueous polyphenol-rich extract (OLE) containing Hydroxytyrosol (0.53mg/L), Luteolin-7-O-glucoside (0.70 mg/L), Apigenin-4-O-glucoside (0.18 mg/L) and Oleuropein (4.24 mg/L) aquatic polyphenols extraction (OLE). Olive leaves, often considered agricultural and industrial waste, hold significant potential for economic and medicinal applications [68,69,72,73]. Previous studies reported the extraction of OLE using different solvent systems. Specifically, Medfai et al obtained an ethanolic OLE, while Oliveira et all obtained OLE by using an ethanol/water hydroalcoholic solvent (70:30, with the addition of about 1% acetic acid in the mixture) for the extraction [69,73]. More recently, Tarchi et al produced an oleuropein rich aqueous extract from Olive Leaves with a TPC values of 395.45 ± 8.21 mg GAE/g via an autoclave method which, although effective, is more complex and costly method than the enzymatic assisted extraction used herein [68]. Following extraction, the OLE was nano-encapsulated in layered double hydroxides (LDHs) by varying the Zn^{2+}/Al^{3+} molar ratio to 1:1, 2:1, and 3:1. Previous encapsulation efforts utilized organic matrices. For example, Medfai et all encapsulated the obtained ethanolic OLE by spray-drying using maltodextrins, maltodextrins–pectin and maltodextrins–gum Arabic as encapsulating

 doi:10.20944/preprints202506.2137.v1

agent [69]. Oliveira et al encapsulated the obtained OLE by using gelatin/tragacanth gum as an encapsulating agent. Tarchi et al encapsulated the rich in oleuropein OLE by using maltodextrin and sodium caseinate as wall materials to preserve the stability and bioavailability of these compounds [68]. In this study is for the first time reported the nano-encapsulation of such OLE in LDH nanocarriers. The obtained OLE@LDH_Zn/Al_1/1, OLE@LDH_Zn/Al_2/1, and OLE@LDH_Zn/Al_3/1 nanohybrids physiochemically characterized via XRD, FTIR and SEM analysis which clearly shown the incorporation of OLE inside the interlayer space of LDHs in all cases to obtain intercalated nanocomposite structures. Both antioxidant and antibacterial activity tests revealed that OLE@LDH_Zn/Al_1/1 nanohybrid has the lowest EC_{50} value (83.64±5.45) and the highest MIC (3.12-1.56 mg/mL) and MBC (12.5-6.25 mg/mL) values against *E. Coli* and *S. Aureus* correspondingly. The antioxidant and antibacterial result align with the highest TPC (606.6±7.0) value also obtained for OLE@LDH_Zn/Al_1/1 nanohybrid. The highest antioxidant antibacterial activity of OLE@LDH_Zn/Al_1/1 nanohybrid in line with its highest TPC capacity exhibited due to its highest positive sheets of LDH which can intercalate more negative charged OLE amount. Thus, in this study not only prepared and characterized for the first time the OLE@LDH_Zn/Al_x/1 nanohybrids but also the optimum Zn^{2+} ions to A^{3+} ions ratio for the encapsulation of such OLE in obtained OLE@LDH_Zn/Al_1/1 nanohybrid was proven. Finally, herein in via the TPC experiments in different pH values clearly shown that the nanoencapsulated OLE is well protected inside the LDH sheets at 7 and 3.6 pH values and release at a pH 1 (pH of stomach) in all cases of obtained OLE@LDH_Zn/Al_x/1 nanohybrids. Overall, it was shown that: (i) LDH seems to be an ideal nanocarrier for the encapsulation of such OLE and their control release under stomach pH conditions, and (ii) the OLE@LDH_Zn/Al_1/1 nanohybrid has a great potential to be used in future nutritional, food preservation and or biomedicine applications.

5. Conclusions

This work introduces an efficient, green valorization strategy for olive leaves via enzymatic-assisted extraction, yielding a polyphenol-rich olive leaf extract (OLE) containing hydroxytyrosol, luteolin-7-O-glucoside, apigenin-4-O-glucoside, and oleuropein. For the first time, this extract was successfully nanoencapsulated into Zn-Al layered double hydroxides (LDHs) at varying Zn^{2+}/Al^{3+} molar ratios. Comprehensive structural and functional characterizations confirmed the formation of intercalated nanohybrids, with the 1:1 Zn/Al ratio (OLE@LDH_Zn/Al_1/1) demonstrating superior performance. This hybrid exhibited the highest total polyphenol content, the strongest antioxidant activity, and the most potent antibacterial effect among the tested formulations. Additionally, pH-responsive release studies verified that OLE polyphenols are effectively protected within the LDH interlayers under neutral and slightly acidic conditions and are released in acidic environments, mimicking gastric pH. These findings establish LDH-based nanohybrids as an effective delivery platform for plant-derived polyphenols and highlight their potential for future applications in food preservation, nutrition, and biomedicine.

Supplementary Materials: The following supporting information can be downloaded at the website of this paper posted on Preprints.org, Figure S1: Obtained calibration curves of (a) Hydroxytyrosol, (b) Luteolin-7-O-glucoside, (c) Apigenin-4-O-glucoside and (d) Oleuropein; Figure S2: HPLC-DAD chromatographic plot at 280 nm for pure OLE; Figure S3: Linear plots used for the calculation of average values of EC_{50}; Figure S4: Results (three repetitions) to determine the minimum bactericidal concentration (MBC) of all OLE@LDH_Zn/Al_x/1 nanohybrids against E. Coli and S. Aureus. Representative images of resazurin-based 96-well plate microdilution method used to determine the minimum bactericidal concentration (MBC) of all OLE@LDH_Zn/Al_x/1 nanohybrids against E. Coli and S. Aureus.; Table S1: Experimental data used for the calculation of obtained average EC_{50} values; Table S2: Statistical analysis results of EC50 values; TableS3: Statistical analysis results of TPC values.

 doi:10.20944/preprints202506.2137.v1

Acknowledgement: Special thanks are expressed to Prof. Skaltsounis Alexios-Leandros, Director of the Laboratory of Valorization of Bioactive Natural Product, Faculty of Pharmacy, University of Athens, for his insightful comments and valuable contribution to this article.

Author Contributions: Conceptualization—C.E.S. and A.E.G.; data curation—A.V., A.A.L., P.St., M.X., P.S., N.C., A.E.G. and C.E.S.; formal analysis—A.K., A.A.L., P.St., C.P., E.P.G., A.E.G., and C.E.S.; investigation—A.K., A.A.L., N.C., M.X., P.S., C.P., E.P.G., C.E.S., and A.E.G.; methodology—A.K., A.A.L., P.St., M.X., P.S., N.C., C.E.S., and A.E.G.; project administration—C.E.S., and A.E.G.; resources—A.K., A.A.L., N.C., C.E.S., and A.E.G.; software—A.V., A.A.L., N.C., C.E.S., and A.E.G.; supervision—C.E.S., and A.E.G.; validation—A.K., A.A.L., N.C., E.P.G., C.E.S., and A.E.G..; visualization—A.K., N.C., C.E.S., and A.E.G.; writing, original draft—N.C., C.E.S., A.E.G. and A.E.G.; writing, review and editing—A.K., N.C., A.A.L., C.E.S., and A.E.G.; All authors have read and agreed to the published version of the manuscript.

Funding: This research received no external funding.

Data Availability Statement: The datasets generated for this study are available on request to the corresponding author.

Conflicts of Interest: The authors declare no conflicts of interest.

References

1. Cooney, R.; de Sousa, D.B.; Fernández-Ríos, A.; Mellett, S.; Rowan, N.; Morse, A.P.; Hayes, M.; Laso, J.; Regueiro, L.; Wan, A.HL.; et al. A Circular Economy Framework for Seafood Waste Valorisation to Meet Challenges and Opportunities for Intensive Production and Sustainability. *J. Clean. Prod.* **2023**, *392*, 136283, doi:10.1016/j.jclepro.2023.136283.
2. Esposito, B.; Sessa, M.R.; Sica, D.; Malandrino, O. Towards Circular Economy in the Agri-Food Sector. A Systematic Literature Review. *Sustainability* **2020**, *12*, 7401, doi:10.3390/su12187401.
3. Hamam, M.; Chinnici, G.; Di Vita, G.; Pappalardo, G.; Pecorino, B.; Maesano, G.; D'Amico, M. Circular Economy Models in Agro-Food Systems: A Review. *Sustainability* **2021**, *13*, 3453, doi:10.3390/su13063453.
4. Panáček, D.; Zdražil, L.; Langer, M.; Šedajová, V.; Baďura, Z.; Zoppellaro, G.; Yang, Q.; Nguyen, E.P.; Álvarez-Diduk, R.; Hrubý, V.; et al. Graphene Nanobeacons with High-Affinity Pockets for Combined, Selective, and Effective Decontamination and Reagentless Detection of Heavy Metals. *Small* **2022**, *18*, 2201003, doi:10.1002/smll.202201003.
5. Rontogianni, A.; Chalmpes, N.; Nikolaraki, E.; Botzolaki, G.; Androulakis, A.; Stratakis, A.; Zygouri, P.; Moschovas, D.; Avgeropoulos, A.; Karakassides, M.A.; et al. Efficient CO2 Hydrogenation over Mono- and Bi-Metallic RuNi/MCM-41 Catalysts: Controlling CH4 and CO Products Distribution through the Preparation Method and/or Partial Replacement of Ni by Ru. *Chem. Eng. J.* **2023**, *474*, 145644, doi:10.1016/j.cej.2023.145644.
6. Cansado, I.P. da P.; Mourão, P.A.M.; Castanheiro, J.E.; Geraldo, P.F.; Suhas; Suero, S.R.; Cano, B.L. A Review of the Biomass Valorization Hierarchy. *Sustainability* **2025**, *17*, 335, doi:10.3390/su17010335.
7. Joshi, N.C.; Sinha, S.; Bhatnagar, P.; Nath, Y.; Negi, B.; Kumar, V.; Gururani, P. A Concise Review on Waste Biomass Valorization through Thermochemical Conversion. *Curr. Res. Microb. Sci.* **2024**, *6*, 100237, doi:10.1016/j.crmicr.2024.100237.
8. Areti, H.A.; Muleta, M.D.; Abo, L.D.; Hamda, A.S.; Adugna, A.A.; Edae, I.T.; Daba, B.J.; Gudeta, R.L. Innovative Uses of Agricultural By-Products in the Food and Beverage Sector: A Review. *Food Chem. Adv.* **2024**, *5*, 100838, doi:10.1016/j.focha.2024.100838.
9. Lai, W.T.; Khong, N.M.H.; Lim, S.S.; Hee, Y.Y.; Sim, B.I.; Lau, K.Y.; Lai, O.M. A Review: Modified Agricultural by-Products for the Development and Fortification of Food Products and Nutraceuticals. *Trends Food Sci. Technol.* **2017**, *59*, 148–160, doi:10.1016/j.tifs.2016.11.014.
10. Ruff, A.J. Food Industry Side Streams: An Unexploited Source for Biotechnological Phosphorus Upcycling. *Curr. Opin. Biotechnol.* **2024**, *90*, 103209, doi:10.1016/j.copbio.2024.103209.
11. Salvatore, I.; Leue-Rüegg, R.; Beretta, C.; Müller, N. Valorisation Potential and Challenges of Food Side Product Streams for Food Applications: A Review Using the Example of Switzerland. *Future Foods* **2024**, *9*, 100325, doi:10.1016/j.fufo.2024.100325.

 doi:10.20944/preprints202506.2137.v1

12. Chalmpes, N.; Tantis, I.; Alsmaeil, A.W.; Aldakkan, B.S.; Dimitrakou, A.; Karakassides, M.A.; Salmas, C.E.; Giannelis, E.P. Elevating Waste Biomass: Supercapacitor Electrode Materials Derived from Spent Coffee Grounds. *Energy Fuels* **2025**, *39*, 1305–1315, doi:10.1021/acs.energyfuels.4c05250.
13. Guillard, V.; Gaucel, S.; Fornaciari, C.; Angellier-Coussy, H.; Buche, P.; Gontard, N. The Next Generation of Sustainable Food Packaging to Preserve Our Environment in a Circular Economy Context. *Front. Nutr.* **2018**, *5*, doi:10.3389/fnut.2018.00121.
14. Gupta, S.; Sharma, S.; Kumar Nadda, A.; Saad Bala Husain, M.; Gupta, A. Biopolymers from Waste Biomass and Its Applications in the Cosmetic Industry: A Review. *Mater. Today Proc.* **2022**, *68*, 873–879, doi:10.1016/j.matpr.2022.06.422.
15. Al-Maqtari, Q.A.; Rehman, A.; Mahdi, A.A.; Al-Ansi, W.; Wei, M.; Yanyu, Z.; Phyo, H.M.; Galeboe, O.; Yao, W. Application of Essential Oils as Preservatives in Food Systems: Challenges and Future Prospectives – a Review. *Phytochem. Rev.* **2022**, *21*, 1209–1246, doi:10.1007/s11101-021-09776-y.
16. Almeida-Souza, F.; Magalhães, I.F.B.; Guedes, A.C.; Santana, V.M.; Teles, A.M.; Mouchrek, A.N.; Calabrese, K.S.; Abreu-Silva, A.L. Safety Assessment of Essential Oil as a Food Ingredient. In *Essential Oils: Applications and Trends in Food Science and Technology*; Santana de Oliveira, M., Ed.; Springer International Publishing: Cham, 2022; pp. 123–171 ISBN 978-3-030-99476-1.
17. Bakkali, F.; Averbeck, S.; Averbeck, D.; Idaomar, M. Biological Effects of Essential Oils – A Review. *Food Chem. Toxicol.* **2008**, *46*, 446–475, doi:10.1016/j.fct.2007.09.106.
18. Salas, E.; Oliveira, J.; Perez-Gregorio, R. Editorial: Natural Extracts as Food Ingredients: From Chemistry to Health. *Front. Nutr.* **2023**, *10*, doi:10.3389/fnut.2023.1306307.
19. Li, J.; Sun, H.; Weng, Y. Natural Extracts and Their Applications in Polymer-Based Active Packaging: A Review. *Polymers* **2024**, *16*, 625, doi:10.3390/polym16050625.
20. Giannakas, A.E. Plant Extracts-Based Food Packaging Films. In *Natural Materials for Food Packaging Application*; John Wiley & Sons, Ltd, 2023; pp. 23–49 ISBN 978-3-527-83730-4.
21. Giannakas, A.E. 7 - Bionanocomposites with Hybrid Nanomaterials for Food Packaging Applications. In *Advances in Biocomposites and their Applications*; Karak, N., Ed.; Woodhead Publishing Series in Composites Science and Engineering; Woodhead Publishing, 2024; pp. 201–225 ISBN 978-0-443-19074-2.
22. Deshmukh, R.K.; Hakim, L.; Akhila, K.; Ramakanth, D.; Gaikwad, K.K. Nano Clays and Its Composites for Food Packaging Applications. *Int. Nano Lett.* **2023**, *13*, 131–153, doi:10.1007/s40089-022-00388-8.
23. Blinka, T.A.; Edwards, F.B.; Miranda, N.R.; Speer, D.V.; Thomas, J.A. Zeolite in Packaging Film 1997.
24. Salmas, C.E.; Giannakas, A.E.; Karabagias, V.K.; Moschovas, D.; Karabagias, I.K.; Gioti, C.; Georgopoulos, S.; Leontiou, A.; Kehayias, G.; Avgeropoulos, A.; et al. Development and Evaluation of a Novel-Thymol@Natural-Zeolite/Low-Density-Polyethylene Active Packaging Film: Applications for Pork Fillets Preservation. *Antioxidants* **2023**, *12*, 523, doi:10.3390/antiox12020523.
25. Kumari, S.; Soni, S.; Sharma, A.; Kumar, S.; Sharma, V.; Jaswal, V.S.; Bhatia, S.K.; Sharma, A.K. Layered Double Hydroxides Based Composite Materials and Their Applications in Food Packaging. *Appl. Clay Sci.* **2024**, *247*, 107216, doi:10.1016/j.clay.2023.107216.
26. Daniel, S.; Thomas, S. 1 - Layered Double Hydroxides: Fundamentals to Applications. In *Layered Double Hydroxide Polymer Nanocomposites*; Thomas, S., Daniel, S., Eds.; Woodhead Publishing Series in Composites Science and Engineering; Woodhead Publishing, 2020; pp. 1–76 ISBN 978-0-08-102261-0.
27. Alexandre, M.; Dubois, P. Polymer-Layered Silicate Nanocomposites: Preparation, Properties and Uses of a New Class of Materials. *Mater. Sci. Eng. R Rep.* **2000**, *28*, 1–63, doi:10.1016/S0927-796X(00)00012-7.
28. Chalmpes, N.; Kouloumpis, A.; Zygouri, P.; Karouta, N.; Spyrou, K.; Stathi, P.; Tsoufis, T.; Georgakilas, V.; Gournis, D.; Rudolf, P. Layer-by-Layer Assembly of Clay–Carbon Nanotube Hybrid Superstructures. *ACS Omega* **2019**, *4*, 18100–18107, doi:10.1021/acsomega.9b01970.
29. de Oliveira, L.H.; Trigueiro, P.; Souza, J.S.N.; de Carvalho, M.S.; Osajima, J.A.; da Silva-Filho, E.C.; Fonseca, M.G. Montmorillonite with Essential Oils as Antimicrobial Agents, Packaging, Repellents, and Insecticides: An Overview. *Colloids Surf. B Biointerfaces* **2022**, *209*, 112186, doi:10.1016/j.colsurfb.2021.112186.
30. Deshmukh, R.K.; Kumar, L.; Gaikwad, K.K. Halloysite Nanotubes for Food Packaging Application: A Review. *Appl. Clay Sci.* **2023**, *234*, 106856, doi:10.1016/j.clay.2023.106856.

 doi:10.20944/preprints202506.2137.v1

31. Singha Roy, A.; Kesavan Pillai, S.; Ray, S.S. Layered Double Hydroxides for Sustainable Agriculture and Environment: An Overview. *ACS Omega* **2022**, *7*, 20428–20440, doi:10.1021/acsomega.2c01405.
32. Ghotbi, M.Y.; Hussein, M.Z. bin; Yahaya, A.H.; Rahman, M.Z.A. LDH-Intercalated d-Gluconate: Generation of a New Food Additive-Inorganic Nanohybrid Compound. *J. Phys. Chem. Solids* **2009**, *70*, 948–954, doi:10.1016/j.jpcs.2009.05.007.
33. Bugatti, V.; Bernardo, P.; Clarizia, G.; Viscusi, G.; Vertuccio, L.; Gorrasi, G. Ball Milling to Produce Composites Based of Natural Clinoptilolite as a Carrier of Salicylate in Bio-Based PA11. *Polymers* **2019**, *11*, 634, doi:10.3390/polym11040634.
34. Mondal, S.; Dasgupta, S.; Maji, K. MgAl- Layered Double Hydroxide Nanoparticles for Controlled Release of Salicylate. *Mater. Sci. Eng. C* **2016**, *68*, 557–564, doi:10.1016/j.msec.2016.06.029.
35. Aisawa, S.; Higashiyama, N.; Takahashi, S.; Hirahara, H.; Ikematsu, D.; Kondo, H.; Nakayama, H.; Narita, E. Intercalation Behavior of L-Ascorbic Acid into Layered Double Hydroxides. *Appl. Clay Sci.* **2007**, *35*, 146–154, doi:10.1016/j.clay.2006.09.003.
36. Rahmanian, O.; Dinari, M.; Neamati, S. Synthesis and Characterization of Citrate Intercalated Layered Double Hydroxide as a Green Adsorbent for Ni2+ and Pb2+ Removal. *Environ. Sci. Pollut. Res.* **2018**, *25*, 36267–36277, doi:10.1007/s11356-018-3584-8.
37. Quintieri, L.; Bugatti, V.; Caputo, L.; Vertuccio, L.; Gorrasi, G. A Food-Grade Resin with LDH–Salicylate to Extend Mozzarella Cheese Shelf Life. *Processes* **2021**, *9*, 884, doi:10.3390/pr9050884.
38. Bugatti, V.; Vertuccio, L.; Zuppardi, F.; Vittoria, V.; Gorrasi, G. PET and Active Coating Based on a LDH Nanofiller Hosting P-Hydroxybenzoate and Food-Grade Zeolites: Evaluation of Antimicrobial Activity of Packaging and Shelf Life of Red Meat. *Nanomaterials* **2019**, *9*, 1727, doi:10.3390/nano9121727.
39. Viscusi, G.; Bugatti, V.; Vittoria, V.; Gorrasi, G. Antimicrobial Sorbate Anchored to Layered Double Hydroxide (LDH) Nano-Carrier Employed as Active Coating on Polypropylene (PP) Packaging: Application to Bread Stored at Ambient Temperature. *Future Foods* **2021**, *4*, 100063, doi:10.1016/j.fufo.2021.100063.
40. Bugatti, V.; Vertuccio, L.; Zara, S.; Fancello, F.; Scanu, B.; Gorrasi, G. Green Pesticides Based on Cinnamate Anion Incorporated in Layered Double Hydroxides and Dispersed in Pectin Matrix. *Carbohydr. Polym.* **2019**, *209*, 356–362, doi:10.1016/j.carbpol.2019.01.033.
41. Nalawade, P.; Aware, B.; Kadam, V.; Hirlekar, R. Layered Double Hydroxides: A Review. *J. Sci. Ind. Res.* **2009**.
42. Mir-Cerdà, A.; Granados, M.; Saurina, J.; Sentellas, S. Olive Tree Leaves as a Great Source of Phenolic Compounds: Comprehensive Profiling of NaDES Extracts. *Food Chem.* **2024**, *456*, 140042, doi:10.1016/j.foodchem.2024.140042.
43. Debs, E.; Abi-Khattar, A.-M.; Rajha, H.N.; Abdel-Massih, R.M.; Assaf, J.-C.; Koubaa, M.; Maroun, R.G.; Louka, N. Valorization of Olive Leaves through Polyphenol Recovery Using Innovative Pretreatments and Extraction Techniques: An Updated Review. *Separations* **2023**, *10*, 587, doi:10.3390/separations10120587.
44. Vardakas, A.; Kechagias, A.; Penov, N.; Giannakas, A.E. Optimization of Enzymatic Assisted Extraction of Bioactive Compounds from Olea Europaea Leaves. *Biomass* **2024**, *4*, 647–657, doi:10.3390/biomass4030035.
45. IOC STANDARDS, METHODS AND GUIDES. *Int. Olive Counc.*
46. Elshikh, M.; Ahmed, S.; Funston, S.; Dunlop, P.; McGaw, M.; Marchant, R.; Banat, I.M. Resazurin-Based 96-Well Plate Microdilution Method for the Determination of Minimum Inhibitory Concentration of Biosurfactants. *Biotechnol. Lett.* **2016**, *38*, 1015–1019, doi:10.1007/s10529-016-2079-2.
47. Boukhalfa, N.; Boutahala, M.; Djebri, N. Synthesis and Characterization of ZnAl-Layered Double Hydroxide and Organo-K10 Montmorillonite for the Removal of Diclofenac from Aqueous Solution. *Adsorpt. Sci. Technol.* **2017**, *35*, 20–36, doi:10.1177/0263617416666548.
48. Ahmed, A.A.A.; Talib, Z.A.; Hussein, M.Z. bin Thermal, Optical and Dielectric Properties of Zn–Al Layered Double Hydroxide. *Appl. Clay Sci.* **2012**, *56*, 68–76, doi:10.1016/j.clay.2011.11.024.
49. Smalenskaite, A.; Pavasaryte, L.; Yang, T.C.K.; Kareiva, A. Undoped and Eu3+ Doped Magnesium-Aluminium Layered Double Hydroxides: Peculiarities of Intercalation of Organic Anions and Investigation of Luminescence Properties. *Materials* **2019**, *12*, 736, doi:10.3390/ma12050736.

 doi:10.20944/preprints202506.2137.v1

50. Khan, A.I.; O'Hare, D. Intercalation Chemistry of Layered Double Hydroxides: Recent Developments and Applications. *J. Mater. Chem.* **2002**, *12*, 3191–3198, doi:10.1039/B204076J.
51. Agatonovic-Kustrin, S.; Gegechkori, V.; Petrovich, D.S.; Ilinichna, K.T.; Morton, D.W. HPTLC and FTIR Fingerprinting of Olive Leaves Extracts and ATR-FTIR Characterisation of Major Flavonoids and Polyphenolics. *Molecules* **2021**, *26*, 6892, doi:10.3390/molecules26226892.
52. Nasir1, G.A.; Mohammed2, A.K.; Samir3, H.F. Biosynthesis and Characterization of Silver Nanoparticles Using Olive Leaves Extract and Sorbitol. *Iraqi J. Biotechnol.* **2016**, *15*.
53. Chalmpes, N.; Bourlinos, A.B.; Talande, S.; Bakandritsos, A.; Moschovas, D.; Avgeropoulos, A.; Karakassides, M.A.; Gournis, D. Nanocarbon from Rocket Fuel Waste: The Case of Furfuryl Alcohol-Fuming Nitric Acid Hypergolic Pair. *Nanomaterials* **2021**, *11*, 1, doi:10.3390/nano11010001.
54. Kouloumpis, A.; Vourdas, N.; Zygouri, P.; Chalmpes, N.; Potsi, G.; Kostas, V.; Spyrou, K.; Stathopoulos, V.N.; Gournis, D.; Rudolf, P. Controlled Deposition of Fullerene Derivatives within a Graphene Template by Means of a Modified Langmuir-Schaefer Method. *J. Colloid Interface Sci.* **2018**, *524*, 388–398, doi:10.1016/j.jcis.2018.04.049.
55. Shameli, K.; Ahmad, M.B.; Jazayeri, S.D.; Shabanzadeh, P.; Sangpour, P.; Jahangirian, H.; Gharayebi, Y. Investigation of Antibacterial Properties Silver Nanoparticles Prepared via Green Method. *Chem. Cent. J.* **2012**, *6*, 73, doi:10.1186/1752-153X-6-73.
56. Khalil, M.M.H.; Ismail, E.H.; El-Baghdady, K.Z.; Mohamed, D. Green Synthesis of Silver Nanoparticles Using Olive Leaf Extract and Its Antibacterial Activity. *Arab. J. Chem.* **2014**, *7*, 1131–1139, doi:10.1016/j.arabjc.2013.04.007.
57. Chalmpes, N.; Patila, M.; Kouloumpis, A.; Alatzoglou, C.; Spyrou, K.; Subrati, M.; Polydera, A.C.; Bourlinos, A.B.; Stamatis, H.; Gournis, D. Graphene Oxide–Cytochrome c Multilayered Structures for Biocatalytic Applications: Decrypting the Role of Surfactant in Langmuir–Schaefer Layer Deposition. *ACS Appl. Mater. Interfaces* **2022**, *14*, 26204–26215, doi:10.1021/acsami.2c03944.
58. Chalmpes, N.; Moschovas, D.; Tantis, I.; Bourlinos, A.B.; Bakandritsos, A.; Fotiadou, R.; Patila, M.; Stamatis, H.; Avgeropoulos, A.; Karakassides, M.A.; et al. Carbon Nanostructures Derived through Hypergolic Reaction of Conductive Polymers with Fuming Nitric Acid at Ambient Conditions. *Molecules* **2021**, *26*, 1595, doi:10.3390/molecules26061595.
59. Mahjoubi, F.Z.; Khalidi, A.; Abdennouri, M.; Barka, N. Zn–Al Layered Double Hydroxides Intercalated with Carbonate, Nitrate, Chloride and Sulphate Ions: Synthesis, Characterisation and Dye Removal Properties. *J. Taibah Univ. Sci.* **2017**, *11*, 90–100, doi:10.1016/j.jtusci.2015.10.007.
60. Chen, X.; Li, H.; Xu, J.; Jaber, F.; Musharavati, F.; Zalnezhad, E.; Bae, S.; Hui, K.S.; Hui, K.N.; Liu, J. Synthesis and Characterization of a NiCo2O4@NiCo2O4 Hierarchical Mesoporous Nanoflake Electrode for Supercapacitor Applications. *Nanomaterials* **2020**, *10*, 1292, doi:10.3390/nano10071292.
61. Hui, L.; Xue, Y.; Huang, B.; Yu, H.; Zhang, C.; Zhang, D.; Jia, D.; Zhao, Y.; Li, Y.; Liu, H.; et al. Overall Water Splitting by Graphdiyne-Exfoliated and -Sandwiched Layered Double-Hydroxide Nanosheet Arrays. *Nat. Commun.* **2018**, *9*, 5309, doi:10.1038/s41467-018-07790-x.
62. Kechagias, A.; Salmas, C.E.; Chalmpes, N.; Leontiou, A.A.; Karakassides, M.A.; Giannelis, E.P.; Giannakas, A.E. Laponite vs. Montmorillonite as Eugenol Nanocarriers for Low Density Polyethylene Active Packaging Films. *Nanomaterials* **2024**, *14*, 1938, doi:10.3390/nano14231938.
63. Wang, Q.; O'Hare, D. Recent Advances in the Synthesis and Application of Layered Double Hydroxide (LDH) Nanosheets. *Chem. Rev.* **2012**, *112*, 4124–4155, doi:10.1021/cr200434v.
64. Mohanty, U.A.; Sahoo, D.P.; Paramanik, L.; Parida, K. A Critical Review on Layered Double Hydroxide (LDH)-Derived Functional Nanomaterials as Potential and Sustainable Photocatalysts. *Sustain. Energy Fuels* **2023**, *7*, 1145–1186, doi:10.1039/D2SE01510B.
65. Ahmed, A.A.A.; Talib, Z.A.; bin Hussein, M.Z.; Zakaria, A. Zn–Al Layered Double Hydroxide Prepared at Different Molar Ratios: Preparation, Characterization, Optical and Dielectric Properties. *J. Solid State Chem.* **2012**, *191*, 271–278, doi:10.1016/j.jssc.2012.03.013.
66. Jakobek, L.; Ištuk, J.; Barron, A.R.; Matić, P. Bioactive Phenolic Compounds from Apples during Simulated In Vitro Gastrointestinal Digestion: Kinetics of Their Release. *Appl. Sci.* **2023**, *13*, 8434, doi:10.3390/app13148434.

 doi:10.20944/preprints202506.2137.v1

67. Li, H.; Gao, Z.; Xu, J.; Sun, W.; Wu, J.; Zhu, L.; Gao, M.; Zhan, X. Encapsulation of Polyphenols in pH-Responsive Micelles Self-Assembled from Octenyl-Succinylated Curdlan Oligosaccharide and Its Effect on the Gut Microbiota. *Colloids Surf. B Biointerfaces* **2022**, *219*, 112857, doi:10.1016/j.colsurfb.2022.112857.
68. Tarchi, I.; Olewnik-Kruszkowska, E.; Aït-Kaddour, A.; Bouaziz, M. Innovative Process for the Recovery of Oleuropein-Rich Extract from Olive Leaves and Its Biological Activities: Encapsulation for Activity Preservation with Concentration Assessment Pre and Post Encapsulation. *ACS Omega* **2025**, *10*, 6135–6146, doi:10.1021/acsomega.4c10858.
69. Medfai, W.; Oueslati, I.; Dumas, E.; Harzalli, Z.; Viton, C.; Mhamdi, R.; Gharsallaoui, A. Physicochemical and Biological Characterization of Encapsulated Olive Leaf Extracts for Food Preservation. *Antibiotics* **2023**, *12*, 987, doi:10.3390/antibiotics12060987.
70. Gajic, I.; Kabic, J.; Kekic, D.; Jovicevic, M.; Milenkovic, M.; Mitic Culafic, D.; Trudic, A.; Ranin, L.; Opavski, N. Antimicrobial Susceptibility Testing: A Comprehensive Review of Currently Used Methods. *Antibiotics* **2022**, *11*, 427, doi:10.3390/antibiotics11040427.
71. Balouiri, M.; Sadiki, M.; Ibnsouda, S.K. Methods for *in Vitro* Evaluating Antimicrobial Activity: A Review. *J. Pharm. Anal.* **2016**, *6*, 71–79, doi:10.1016/j.jpha.2015.11.005.
72. Paciulli, M.; Grimaldi, M.; Rinaldi, M.; Cavazza, A.; Flamminii, F.; Mattia, C.D.; Gennari, M.; Chiavaro, E. Microencapsulated Olive Leaf Extract Enhances Physicochemical Stability of Biscuits. *Future Foods* **2023**, *7*, 100209, doi:10.1016/j.fufo.2022.100209.
73. Oliveira, F.M.; Oliveira, R.M.; Gehrmann Buchweitz, L.T.; Pereira, J.R.; Cristina dos Santos Hackbart, H.; Nalério, É.S.; Borges, C.D.; Zambiazi, R.C. Encapsulation of Olive Leaf Extract (*Olea Europaea* L.) in Gelatin/Tragacanth Gum by Complex Coacervation for Application in Sheep Meat Hamburger. *Food Control* **2022**, *131*, 108426, doi:10.1016/j.foodcont.2021.108426.